

Lasers in Manufacturing Conference 2019

## n- and p-type laser doping of Si thin film transistors coated with chemical solution for CMOS circuit fabrication

Kaname Imokawa<sup>a,b\*</sup>, Takayuki Kurashige<sup>a</sup>, Nozomu Tanaka<sup>a</sup>,  
Akira Suwa<sup>a</sup>, Daisuke Nakamura<sup>a</sup>, Taizoh Sadoh<sup>a</sup>, Tetsuya Goto<sup>c</sup>,  
and Hiroshi Ikenoue<sup>a,b</sup>

<sup>a</sup>Graduate School of Information Science and Electrical Engineering, Kyushu University, Fukuoka, Japan

<sup>b</sup>Department of Gigaphoton Next GLP, Kyushu University, Fukuoka, Japan

<sup>c</sup>New Industry Creation Hatchery Center, Tohoku University, Sendai, Japan

---

### Abstract

We demonstrated that p- and n- type activation layer can be formed on crystallized Si thin films by KrF excimer laser doping.  $\text{H}_3\text{PO}_4$  (n-type) solution and  $\text{Al}_2\text{O}_3$  (p-type) sol were coated on the surface of Si as dopant sources. Phosphorus and aluminum concentrations were found to be over  $10^{19}$  on the surface, and their depth profiles were uniform in the Si films. Thus, the technique of laser doping is promising for contact formation in the source/drain of Si thin-film-transistors (TFTs) at a low cost. In this study, the electric characteristics of n-MOS and p-MOS TFTs fabricated by laser doping are presented for CMOS circuit fabrication.

Keywords: Laser Doping; KrF Excimer Laser; Low-temperature-poly-Si; Flexible Display; Thin-Film Transistor;

---

### 1. Introduction

Low-temperature poly-Si (LTPS) is widely used as a channel material in thin-film transistors (TFTs) in flat panel displays (FPDs). LTPS facilitates the high-definition and high-speed operation of FPDs owing to their higher electron mobility (10–100 times) compared with that of amorphous-Si (a-Si). In addition, LTPS can be used in complementary metal-oxide-semiconductor (CMOS) circuits, and they are useful in the integration of peripheral circuits on glass substrates. Therefore, LTPS is expected to be an important material for logic devices on glass substrates. LTPS is formed by excimer laser annealing (ELA). This process can be used to form poly-Si through the crystallization of a-Si, and it is expected to be applied to flexible displays owing to

\* Corresponding author. Tel.: +81-801-784-2568 ;  
E-mail address: kaname\_imokawa@gigaphoton.com .

the low temperature required of this process. Meanwhile, high-temperature processes ( $\sim 500^\circ\text{C}$ ) such as ion implantation and thermal annealing, are essential for low contact resistivity in the source/drain contact of TFTs. In particular, a lower contact resistivity ( $\sim 10^{-6} \Omega\cdot\text{cm}^2$  for n-type,  $\sim 10^{-5} \Omega\cdot\text{cm}^2$  for p-type) is required for the low power consumption of display devices.

However, plastic substrates, which are receiving considerable attention as materials for flexible displays, typically exhibit heat resistances less than  $\sim 200^\circ\text{C}$  [1]. Therefore, higher temperature processes over  $200^\circ\text{C}$  cannot be applied for the manufacturing of flexible displays. Recently, laser doping has been studied to realize doping without a large vacuum chamber and a high-temperature annealing oven [2-4]. In particular, KrF excimer laser (248 nm) exhibits notable features of high output energy and high efficiency, which are typically required for annealing. In addition, a-Si can be melted during the short pulse ( $\sim\text{ns}$ ) of the laser, and dopant sources can diffuse sufficiently into Si [1].

In our previous study, we reported that the laser doping of phosphorus to poly-Si thin films can be achieved using excimer laser irradiation in a phosphoric acid solution [5]. Using this method, it was shown that the implantation and activation of dopants could be performed simultaneously at low temperature. However, this process presented some challenges. First, cavitation bubbles were generated on the irradiated area in the solution during the irradiation process; the laser-irradiation damage of poly-Si was induced by the optical scattering of the laser light at the bubble/solution interface. Next, this method was expensive because of the large amounts of phosphoric acid solution consumed. We overcome these problems by coating the surface of poly-Si with  $\text{H}_3\text{PO}_4$  solution or  $\text{Al}_2\text{O}_3$  sol. Using this novel approach, it was shown that phosphorus and aluminum can be implanted and activated with a low damage to the Si surface. In this study, we report the fundamental properties of doped poly-Si, such as resistivity, reflected light intensity, carrier concentration, and activation ratio. Further, we demonstrate the IV transfer of the top gate transistors (n-MOS and p-MOS) fabricated by laser doping. We demonstrate that the laser doping of crystallized Si is an advantageous technique for significantly simplifying LTPS TFT fabrication.

## 2. Experiments

Figure 1 (a) shows a schematic of the KrF-excimer laser (Gigaphoton Inc., wavelength: 248 nm, pulse duration (full width at half-maximum (FWHM)): 10 ns) doping system, and Fig. 1 (b) shows a schematic of laser doping. The sample is composed of a-Si (50 nm)/ $\text{SiO}_2$  (100 nm)/SiN (50 nm)/ on a quartz substrate. The a-Si films were deposited using low-pressure chemical vapor deposition (CVD). Laser crystallization was conducted at the fluence of  $400 \text{ mJ}/\text{cm}^2$  and 20 shots. Then,  $\text{H}_3\text{PO}_4$  solution or  $\text{Al}_2\text{O}_3$  sol was coated as follows. The coating process was as follows: (1) diluted-hydrofluoric-acid cleaning (10 s), (2) pure-water cleaning, (3) ultraviolet (UV) treatment (10 s), (4) dipping into  $\text{H}_3\text{PO}_4$  solution or  $\text{Al}_2\text{O}_3$  sol (10 s), and (5) pure-water cleaning (10 s). The UV treatment in step (3) was performed using KrF excimer laser irradiation ( $100 \text{ mJ}/\text{cm}^2$ , and 20 shots). This UV laser treatment enhanced the hydrophilicity of the surface of the a-Si film. The pure-water cleaning in step (5) removed any excess  $\text{H}_3\text{PO}_4$  solution or  $\text{Al}_2\text{O}_3$  sol.

The shot repetition rate of the laser was 100 Hz, while the spot size on the surface of the sample was  $800 \mu\text{m} \times 500 \mu\text{m}$ . The sample was scanned in the short-axis direction of the laser beam; the number of laser shots was fixed at 20 per location. A continuous-wave (CW) laser with a wavelength of 640 nm was used to probe the center of the region irradiated by the KrF excimer laser. The reflected probe light from the poly-Si surface was monitored using a photo-detector during the laser irradiation. After the irradiation process, the specific resistivity, depth profiles of the phosphorus and aluminum concentration, carrier concentration, mobility, and activation ratio of poly-Si were measured. The specific resistivity was determined from the sheet resistance (measured by a four-point probe) and the film thickness (50 nm). The phosphorus and aluminum depth profiles were measured using secondary-ion mass spectrometry (SIMS); in addition, the Hall

coefficient and temperature dependence of the conductivity of the Si were measured to evaluate the carrier concentration, mobility, and activation ratio. The contact resistivity of the doped Si was investigated with Al/Ti electrodes using the transmission line model (TLM) method. Finally, the characteristics of n-MOS and p-MOS TFTs fabricated by laser doping are shown.

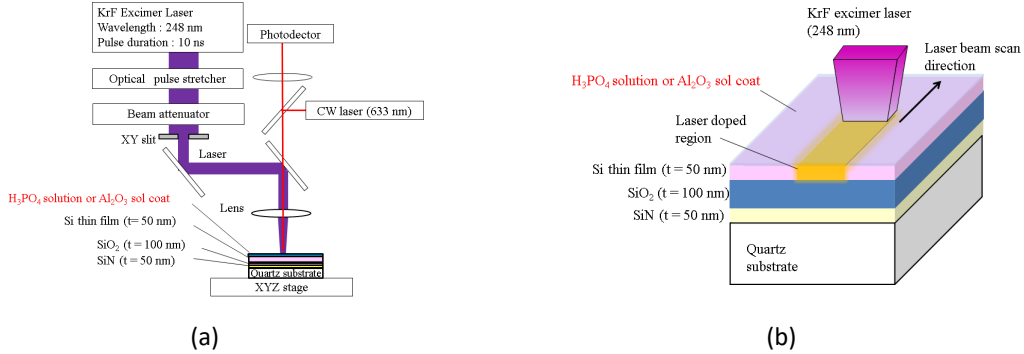


Fig. 1. (a) Schematic of the excimer-laser doping setup and an in-situ observation system, (b) Schematics of laser doping with a coating of chemical solution.

### 3. Results

Figure 2 (a) shows an optical microscopy image of doped Si and Fig. 2 (b) shows the specific resistivity of the Si doped with H<sub>3</sub>PO<sub>4</sub> solution coating (blue line) and Al<sub>2</sub>O<sub>3</sub> sol coating (red line) at different fluences up to 500 mJ/cm<sup>2</sup> and 20 shots. The minimum resistivity value was ~0.08 Ω·cm at 400 mJ/cm<sup>2</sup> with both coatings. The relationship between the specific resistivity and impurity concentration indicates that the lower resistivity is equivalent to the higher concentration [6], and is consistent with the reported value. Thus, these results indicate that phosphorus and aluminum were doped into Si.

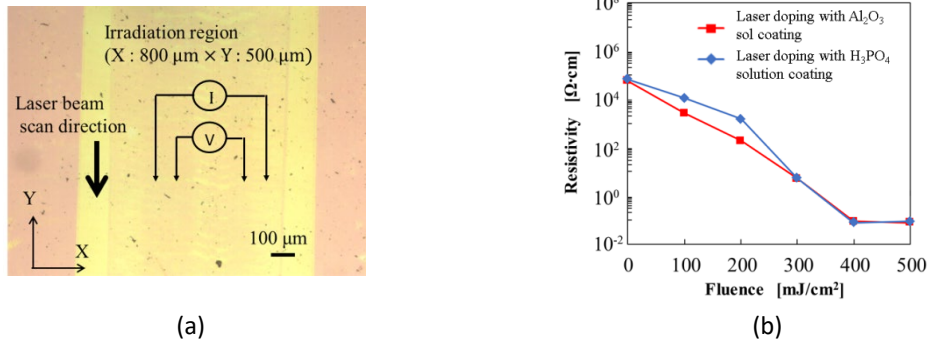


Fig. 2. (a) Optical microscopy image of the doped Si, (b) Resistivity at different fluences up to 500 mJ/cm<sup>2</sup> and 20 shots.

Figure 3 (a) shows the time dependence of the intensity of reflected-light of the CW laser (blue line) and the laser pulse waveform (red line) by laser doping with H<sub>3</sub>PO<sub>4</sub> solution coating at 400 mJ/cm<sup>2</sup> and 1 shot. As evident from this figure, four state changes of Si are considered. Region A shows no irradiation effect. Region B shows the effect of the absorption of laser light and partial melting. This was determined because the intensity of the reflected light was partly reduced. Region C shows the complete melting of the Si surface, because the intensity of the reflected light is saturated. Region D shows the cooling and recrystallization of Si.

Figures 3 (b) and (c) show the resistivity (black dot line) and the maximum intensity of the reflected light of the poly-Si (red line) doped with  $\text{H}_3\text{PO}_4$  solution and  $\text{Al}_2\text{O}_3$  sol coating as a function of laser fluence. The maximum intensity of the reflected light increased and was saturated beyond  $400 \text{ mJ/cm}^2$ . This shows that poly-Si changes from a partial melt to a complete melt at the doped area. Implantation and activation can be performed simultaneously with the complete melting of poly-Si.

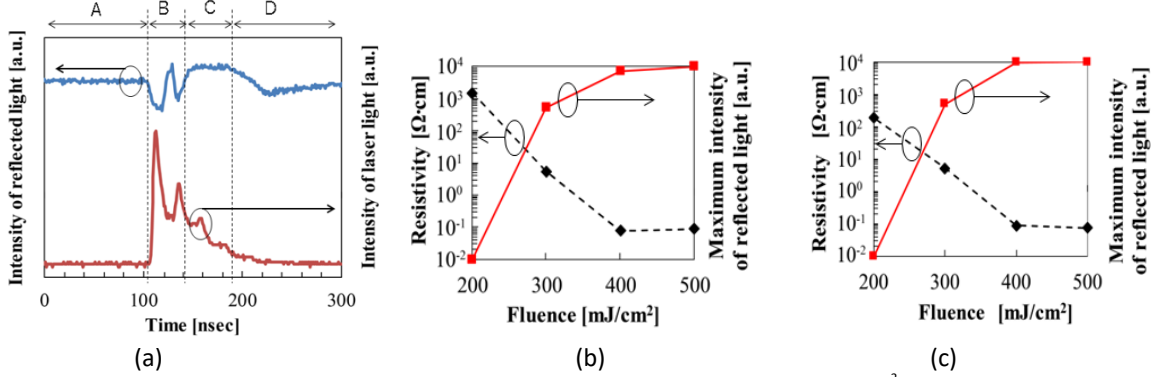


Fig. 3. (a) Reflected-light intensity of Si (blue) and laser pulse waveform (red) versus time at  $400 \text{ mJ/cm}^2$  and 1 shot. (b), (c) Resistivity and maximum intensity of the reflected light as a function of the laser fluence ((b) :  $\text{H}_3\text{PO}_4$ , (c) :  $\text{Al}_2\text{O}_3$ )

Figure 4 (a) and (b) shows the phosphorus and aluminum depth profiles measured by SIMS after laser doping at  $400 \text{ mJ/cm}^2$  and 20 shots. The phosphorus and aluminum concentration in the poly-Si films were found to be uniform (over  $10^{19} \text{ cm}^{-3}$ ). We consider that the diffusion of phosphorus (aluminum) in silicon is sufficient in a short melt time ( $\sim \text{ns}$  order). In addition, the carrier mobility ( $\mu$ ) of the poly-Si film after laser doping was found to be  $61 \text{ cm}^2/\text{Vs}$  (at  $\text{H}_3\text{PO}_4$  condition) and  $13 \text{ cm}^2/\text{Vs}$  (at  $\text{Al}_2\text{O}_3$  condition) at  $400 \text{ mJ/cm}^2$  and 20 shots as obtained by Hall-effect measurements. The carrier concentrations ( $n$ ) were  $1.5 \times 10^{18} \text{ cm}^{-3}$  (at  $\text{H}_3\text{PO}_4$  condition) and  $8.9 \times 10^{18} \text{ cm}^{-3}$  (at  $\text{Al}_2\text{O}_3$  condition). This is one order of magnitude smaller than the impurity concentrations. The most probable reason for this is that carrier traps were produced by laser irradiation and crystal defects.

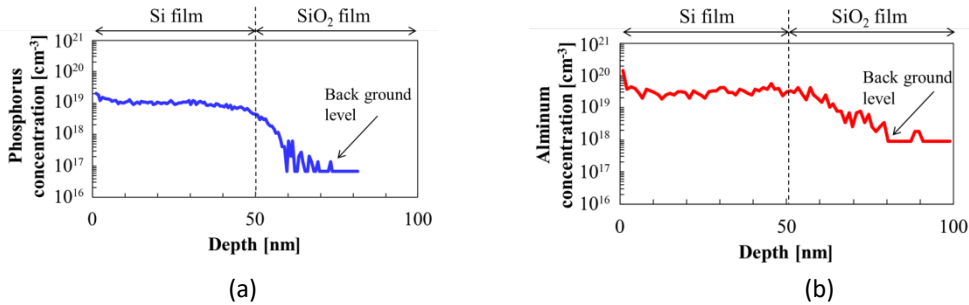


Fig. 4. Depth profiles of phosphorus (a) and aluminum (b) in laser-doped region of Si film at  $400 \text{ mJ/cm}^2$  and 20 shots.

Figure 5 (a) shows a band model of poly-crystalline Si films [7] and Fig. 5 (b) shows the temperature dependence of the conductivity of Si doped with  $\text{H}_3\text{PO}_4$  solution coating at  $400 \text{ mJ/cm}^2$  and 20 shots to estimate the trapped carrier concentration  $Q_t/L$  [ $\text{cm}^{-3}$ ] and donor concentration  $N$  [ $\text{cm}^{-3}$ ];  $Q_t$  [ $\text{cm}^{-2}$ ] is the trap state density per unit area and  $L$  [cm] is the average grain size. Here, the theoretical calculations are shown in Eq. (1)–(3) [7].  $Q_t/L$  calculated based on the conductivity results was  $3.1 \times 10^{17} \text{ cm}^{-3}$ , and the potential

barrier height  $E_B$  was 58 meV. Therefore, a donor concentration of  $1.8 \times 10^{18} \text{ cm}^{-3}$  and carrier activation ratio of 18.1% were obtained from the phosphorus concentration by SIMS, carrier concentration ( $n$ ) by Hall measurements, and trapped carrier concentration  $Q_t/L$ . This result indicates that 17% of carriers were trapped by grain boundaries.

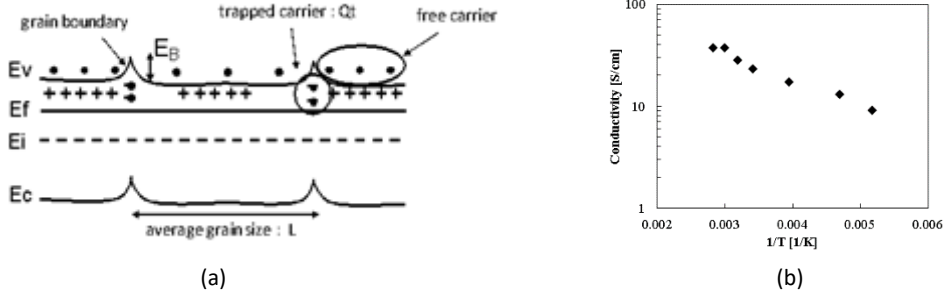


Fig. 5. (a) Band model of poly-crystalline Si films in the case of  $N > Q_t/L$

(b) Temperature dependence of the conductivity in phosphorus-doped region at  $400 \text{ mJ/cm}^2$  and 20 shots.

$$\sigma = Lqn \left( \frac{1}{2\pi m^* kT} \right)^{\frac{1}{2}} \exp\left(-\frac{E_B}{kT}\right) \quad (1)$$

$$E_B = \frac{q^2 Q_t^2}{8\epsilon N} \quad (2)$$

$$n = N \left\{ \left( 1 - \frac{Q_t}{LN} \right) + \frac{1}{qL} \left( \frac{2\epsilon kT\pi}{N} \right)^2 \operatorname{erf} \left[ \frac{qQ_t}{2} \left( \frac{1}{2\epsilon kTN} \right)^{\frac{1}{2}} \right] \right\} \quad (3)$$

Figure 6 (a) shows the optical microscopy image of the phosphorus doped Si captured at  $400 \text{ mJ/cm}^2$  and 20 shots patterned with Al/Ti electrodes on a doped region. Figure 6 (b) shows the resistance between the tungsten probes connected to the phosphorus doped region at different distances between the Al/Ti electrodes on the surface of Si. The contact resistivity ( $\rho_c [\Omega \cdot \text{cm}^2]$ ) of Si with Al/Ti electrodes was estimated using the TLM. Calculations based on the TLM indicated the contact resistivity to be  $8.5 \times 10^{-5} \Omega \cdot \text{cm}^2$  after  $400^\circ \text{C}$  annealing in  $\text{H}_2$  gas. This value is slightly larger than the contact resistivity of Si fabricated by ion implantation, probably owing to the insufficient carrier concentration owing to laser-irradiation-induced crystal defects.

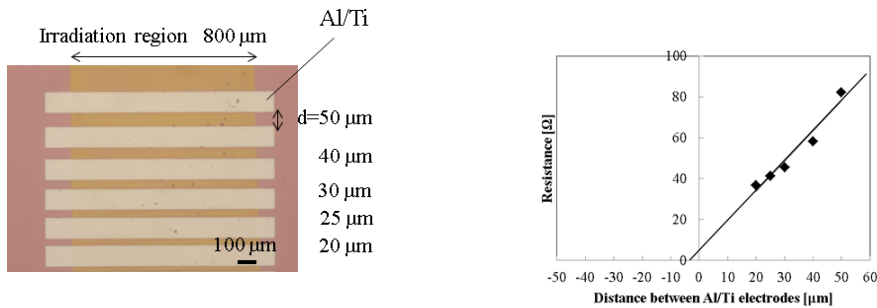


Fig. 6. (a) Optical microscopy image of the phosphorus doped Si with Al/Ti electrodes at  $400 \text{ mJ/cm}^2$  and 20 shots, (b) Resistance between tungsten probes connected to the phosphorus doped region from  $20 \mu\text{m}$  to  $50 \mu\text{m}$  between Al/Ti electrodes.

Figure 7 shows a schematic of the top gate transistor fabrication process. The process flow is shown as follows. First, a-Si (50 nm) films were deposited onto a quartz substrate by low-pressure CVD at 550 °C. Subsequently, ELA was conducted at a fluence range of 400 mJ/cm<sup>2</sup> and 20 shots. After laser irradiation and poly-crystallization, the Si film was patterned by photolithography and wet etched with a mixture of HF, HNO<sub>3</sub>, and H<sub>2</sub>O. For the gate insulator, a SiO<sub>2</sub> film (100 nm) was deposited and contact holes were opened at source/drain regions with buffered HF. The coating process with H<sub>3</sub>PO<sub>4</sub> solution or Al<sub>2</sub>O<sub>3</sub> sol and laser doping at 400 mJ/cm<sup>2</sup> and 20 shots were performed. Then, the gate insulator of the SiO<sub>2</sub> film was removed with buffered HF. The SiO<sub>2</sub> film was re-deposited, and TiN (150 nm) electrode film was deposited and patterned. Next, the dielectric film of SiO<sub>2</sub> (~200 nm) was deposited by atmospheric pressure CVD at 400 °C. The contact holes were opened by wet etching, and the contact metal of Al films were deposited and patterned. Finally, H<sub>2</sub> sintering was performed at 400 °C for 0.5 h.

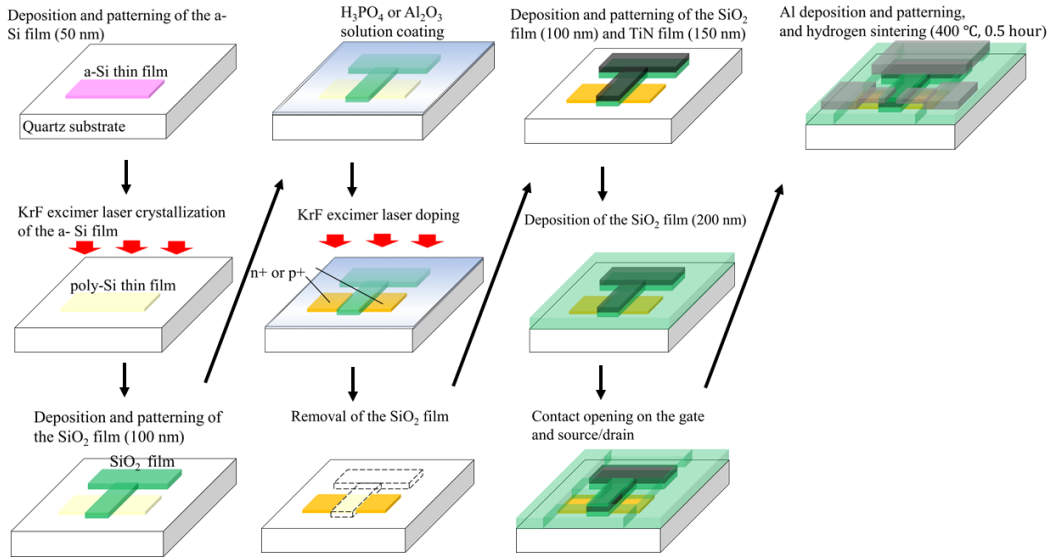


Fig. 7. Schematics of the top gate transistor fabrication process by laser doping with a coating of chemical solution.

Figure 8 shows the transfer curves (drain current ( $I_D$ )–gate voltage ( $V_G$ ) characteristics) of the top gate TFTs fabricated by laser doping with H<sub>3</sub>PO<sub>4</sub> solution (n-MOS) and Al<sub>2</sub>O<sub>3</sub> sol (p-MOS). It was confirmed that TFTs were successfully operated with both chemical coatings. Here, the field-effect mobility ( $\mu_{FE}$ ) in the linear region is based on the transfer curves, and the equation for  $\mu_{FE}$  is as follows:

$$\mu_{FE} = \frac{L}{W} \frac{1}{C_i V_D} \left( \frac{\partial I_D}{\partial V_G} \right) \quad (4)$$

where  $L$  is the length of the channel (20  $\mu\text{m}$ ),  $W$  is the width of the channel (30  $\mu\text{m}$ ), and  $C_i$  is the gate oxide capacitance ( $3.5 \times 10^{-8} \text{ F/cm}^2$ ). The mobility was calculated to be 71 cm<sup>2</sup>/Vs for the n-MOS transistor and 9 cm<sup>2</sup>/Vs for the p-MOS transistor. These values are consistent with the previous measured mobility of 61 cm<sup>2</sup>/Vs (at H<sub>3</sub>PO<sub>4</sub> condition) and 13 cm<sup>2</sup>/Vs (at Al<sub>2</sub>O<sub>3</sub> condition) from the Hall coefficient. Thus, these results are useful for CMOS inverter operation.

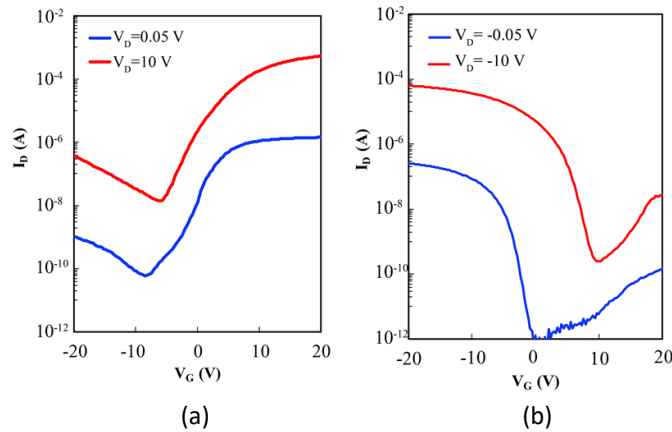


Fig. 8. Transfer curves of the top gate TFTs fabricated by laser doping with  $\text{H}_3\text{PO}_4$  solution (a) and  $\text{Al}_2\text{O}_3$  sol (b).

#### 4. Conclusions

We demonstrated that dopant implantation and activation could be performed simultaneously using KrF excimer laser irradiation and the complete melt of Si thin films coated with  $\text{H}_3\text{PO}_4$  solution or  $\text{Al}_2\text{O}_3$  sol. In addition, we presented the top gate transistors of n-MOS and p-MOS with reasonable mobility. Although a lower contact resistivity was required for practical use, we foresee laser doping to be an effective process for the fabrication of LTPS TFTs. Furthermore, laser doping can potentially be applied to the CMOS TFT fabrication of flexible displays owing to its low-temperature process.

#### Acknowledgements

We would like to express our sincere gratitude to Gigaphoton Inc. for their cooperation in this research. The TFTs were fabricated at fluctuation free facility of New Industry Creation Hatchery Center, Tohoku University.

#### References

- [1] Boyce, J.B., Mei, P., Fulks, R.T., 1998. Laser Processing of Polysilicon Thin Film Transistors: Grain Growth and Device Fabrication, *Physics State Solid* 166, pp. 729-741.
- [2] Smith, P.M., Carey, P.G., Sigmon, T.W., 1997. Excimer Laser Crystallization and Doping Of Silicon Films on Plastic Substrates, *Applied Physics Letters* 70, pp. 342-344.
- [3] Kerrien, G., Sarnet, T., Debarre, D., Boulmer, J., Hernandez, M., Laviron, C., Semeria, M.-N., 2004. Gas Immersion Laser Doping (GILD) for Ultra-Shallow Junction Formation, *Thin Solid Films* 453-454, pp. 106-109.
- [4] Poulain, G., Blanc, D., Focsa, A., Gibier, J., Fourmond, E., Bazer-Bachi, B., Semmache, B., Pellegrin, Y., Lemiti, M., 2012. Selective Laser Doping From Boron Silicate Glass, *Energy Procedia* 27, pp. 455-459.
- [5] Suwa, A., Tanaka, N., Sadoh, T., Nakamura, D., Ikenoue, H., 2017. Characterization of Si Thin Films Doped by Wet Chemical Laser Processing, *J. SID* 48, pp. 430-432.
- [6] M. M. Mandurah, K. C. Saraswat, T. I. Kamins, 1979. Phosphorus Doping of Low Pressure Chemically Vapor-Deposited Silicon Films, *Journal of Electrochemical Society* 126, pp. 1019-1023.
- [7] Seto, J.W.Y., 1975. The Electrical Properties of Polycrystalline Silicon Films, *Journal of Applied Physics* 46, p. 12.